

Neural bases for addictive properties of benzodiazepines

Kelly R. Tan¹, Matthew Brown^{1*}, Gwenaël Labouèbe^{1*}, Cédric Yvon^{1*}, Cyril Creton¹, Jean-Marc Fritschy², Uwe Rudolph³ & Christian Lüscher^{1,4,5}

Benzodiazepines are widely used in clinics and for recreational purposes, but will lead to addiction in vulnerable individuals. Addictive drugs increase the levels of dopamine and also trigger long-lasting synaptic adaptations in the mesolimbic reward system that ultimately may induce the pathological behaviour. The neural basis for the addictive nature of benzodiazepines, however, remains elusive. Here we show that benzodiazepines increase firing of dopamine neurons of the ventral tegmental area through the positive modulation of GABA_A (γ-aminobutyric acid type A) receptors in nearby interneurons. Such disinhibition, which relies on α1-containing GABA_A receptors expressed in these cells, triggers drug-evoked synaptic plasticity in excitatory afferents onto dopamine neurons and underlies drug reinforcement. Taken together, our data provide evidence that benzodiazepines share defining pharmacological features of addictive drugs through cell-type-specific expression of α1-containing GABA_A receptors in the ventral tegmental area. The data also indicate that subunit-selective benzodiazepines sparing α1 may be devoid of addiction liability.

Addictive drugs can be classified into three groups, according to the cellular mechanism through which they increase mesolimbic dopamine (DA)¹. Opioids, cannabinoids and the club drug γ-hydroxybutyrate reduce release from inhibitory afferents onto DA neurons, through their respective G-protein-coupled receptors on GABA neurons. These substances activate pre- and postsynaptic receptors, indirectly increasing the firing rate of DA neurons, a mechanism defined as disinhibition. Nicotine, as a member of the second group, directly depolarizes DA neurons by activating α₄β₂-containing acetylcholine receptors, whereas the third group targets DA transporters (for example, cocaine and amphetamines). It remains unclear whether these mechanisms can account for the addiction liability of benzodiazepines (BDZs)², which are positive modulators of GABA_A receptor (GABA_AR) function.

As well as increasing mesolimbic DA, another common feature of all addictive drugs studied so far is that they trigger adaptive synaptic plasticity in the ventral tegmental area (VTA)³. Hours after the initial exposure, excitatory afferents onto DA neurons of the VTA are strengthened, in part by the insertion of GluR2-lacking AMPARs (α-amino-3-hydroxy-5-methyl-4-isoxazole propionic acid receptors)^{4–6}. To test whether a similar mechanism is elicited by BDZs, we examined whether a single injection of BDZ would, as well as causing an increase in the AMPA/NMDA ratio⁷, also induce a change in the slope of the current–voltage (*I*–*V*)-curve of evoked excitatory postsynaptic currents (EPSCs). Such rectification reflects the presence of GluR2-lacking AMPARs, which are calcium permeable and blocked by polyamines at positive potentials.

BDZ-evoked plasticity in dopamine neurons

In slices obtained 24 h after the intraperitoneal (i.p.) injection of midazolam (MDZ), diazepam or flunitrazepam, the rectification index (RI = EPSC_{–65 mV}/EPSC_{+35 mV}) was significantly higher than in slices from saline-injected controls (Fig. 1a and Supplementary Fig. 2). Similar rectification was measured after an injection of morphine, a member of

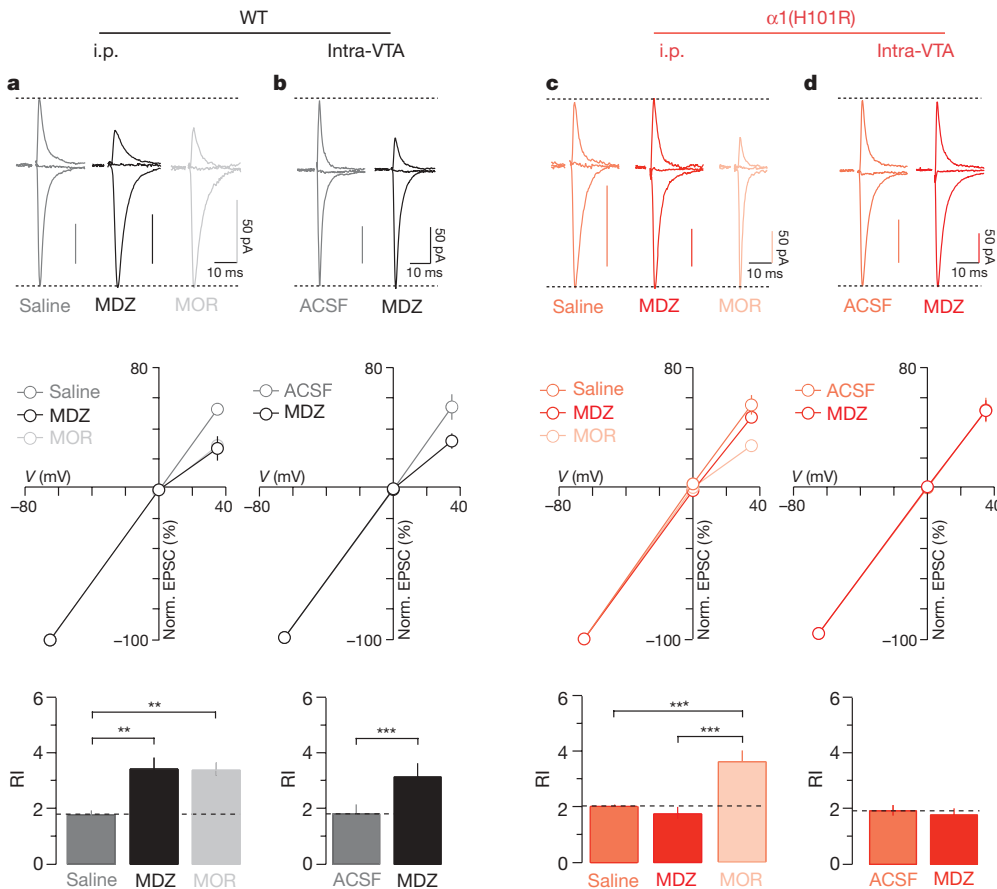
the class of drugs that cause disinhibition of DA neurons⁸. The BDZ antagonist flumazenil blocked rectification when co-injected with MDZ, but was without effect when co-injected with a control saline solution (Fig. 2 and Supplementary Fig. 2). The adaptive plasticity induced by systemic BDZs was also observed 24 h after local application of MDZ into the VTA by stereotactic injection (0.5 μl of an 8 mg ml^{–1} solution over 10 min; Fig. 1b). Thus, BDZ-dependent effects on VTA circuitry are sufficient to induce this cellular hallmark of addictive drugs.

BDZs bind to GABA_ARs at the interface between α and γ subunits⁹ in a subunit-dependent manner. GABA neurons in many parts of the brain express the α1 subunit isoform¹⁰, whereas midbrain DA neurons lack α1 but express α2, α3 and α4 subunit isoforms¹¹. Thus, the addictive potential of BDZs might rely on the potentiation of α1-containing GABA_ARs, which would selectively inhibit GABA neurons and lead to disinhibition of DA neurons. To test this idea, we examined whether MDZ (that is, a rapidly acting, non-selective BDZ with a very strong brain uptake¹²) has an effect in mice with a point mutation (H101R) in the α1 subunit that disrupts the site where BDZs normally bind¹³. In α1(H101R) mice, an i.p. MDZ injection no longer had an effect on the rectification index of AMPAR EPSCs in DA neurons (Fig. 1c). This was not due to a general loss of adaptive plasticity, as morphine still caused a strong rectification. Moreover, stereotactic injections of MDZ into the VTA also failed to elicit rectifying AMPAR-mediated EPSCs in α1(H101R) mice, whereas control injections of artificial cerebrospinal fluid (ACSF) were without effect in either genotype (Fig. 1d). Furthermore, i.p. injection of MDZ increased the AMPA/NMDA ratio in wild-type but not in α1(H101R) mice (Supplementary Fig. 3).

We next used pharmacological tools to confirm the involvement of α1. Zolpidem (ZOL) is a non-classical BDZ selective for α1-containing GABA_ARs¹⁴, whereas the experimental compound L-838 417 does not modulate receptors that contain α1 (ref. 15). We therefore tested whether ZOL and L-838 417 could evoke synaptic plasticity in DA

¹Department of Basic Neurosciences, Medical Faculty, University of Geneva, CH-1211 Geneva, Switzerland. ²Institute of Pharmacology and Toxicology, University of Zurich, CH-8057 Zurich, Switzerland. ³Laboratory of Genetic Neuropharmacology, McLean Hospital and Department of Psychiatry, Harvard Medical School, Belmont, Massachusetts 02478, USA. ⁴Clinic of Neurology, Department of Clinical Neurosciences, Geneva University Hospital, CH-1211 Geneva, Switzerland. ⁵Geneva Neuroscience Center, CH-1211 Geneva, Switzerland.

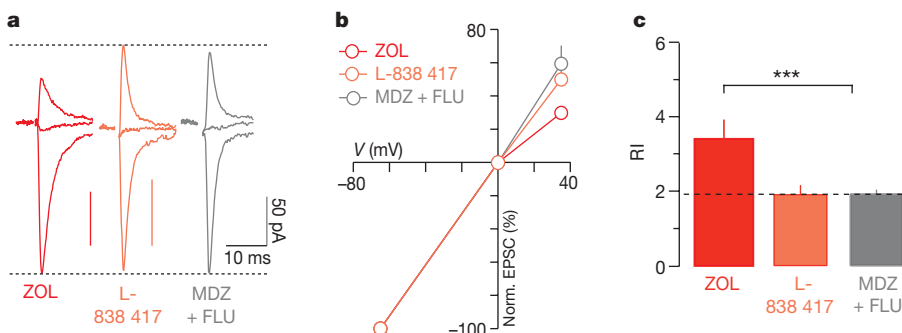
*These authors contributed equally to this work.



neurons. We found that a single injection of ZOL led to rectifying AMPAR-mediated EPSCs, whereas L-838 417 did not affect the $I-V$ curve (Fig. 2). Taken together with the results in $\alpha 1(H101R)$ mice described earlier, we conclude that BDZ-evoked synaptic plasticity depends on $\alpha 1$ -containing GABA_ARs within the VTA.

Cell type-specific expression of $\alpha 1$

To identify $\alpha 1$ -expressing cells in the VTA, we next carried out immunohistochemical staining for tyrosine hydroxylase and the $\alpha 1$ subunit isoform in GAD67 green fluorescent protein (GFP) mice (Fig. 3a). These experiments confirmed that $\alpha 1$ was expressed mainly in GFP-positive neurons, but not in tyrosine-hydroxylase-positive DA neurons. Quantification showed that 81% of the GABA neurons contained the $\alpha 1$ subunit isoform, although this was only the case in 7% of the DA neurons (Fig. 3a, inset). We also observed $\alpha 1$ -staining that could neither be associated to tyrosine-hydroxylase-positive nor GAD67-GFP-expressing cells. This may reflect the pool of the so-called tertiary cells that are neither DA- nor GABA-neurons^{16,17}, or could be due to detectability limits in fine processes.



To assess the functional consequences of this cell-type-specific isoform expression for inhibitory transmission, we characterized miniature inhibitory postsynaptic currents (mIPSCs) in the presence of the glutamate receptor blocker kynurenic acid to isolate GABA_AR-mediated currents (Fig. 3b, c). On average, mIPSCs in GABA neurons were slower and bigger than those in DA neurons, leading to a significantly larger charge transfer in the former (Fig. 3d). This difference was of similar magnitude in wild-type and $\alpha 1(H101R)$ mice (Supplementary Fig. 4), in line with previous reports¹³ that baseline transmission in mutant mice is normal. Moreover, the frequency of mIPSCs, as well as the multiplicity factor (Supplementary Fig. 4c and see Methods for detailed description), were similar in GABA and DA neurons in both genotypes. Although this approach has its limitations¹⁸, it suggests that the number of inhibitory synapses is in the same range in the two cell types. To confirm further that synapses on GABA neurons express $\alpha 1$ -containing GABA_ARs, we tested for effects of MDZ on charge transfer and frequency of mIPSCs in wild-type and $\alpha 1(H101R)$ mice. In DA neurons, MDZ significantly increased the charge transfer and decreased the mIPSC frequency in both

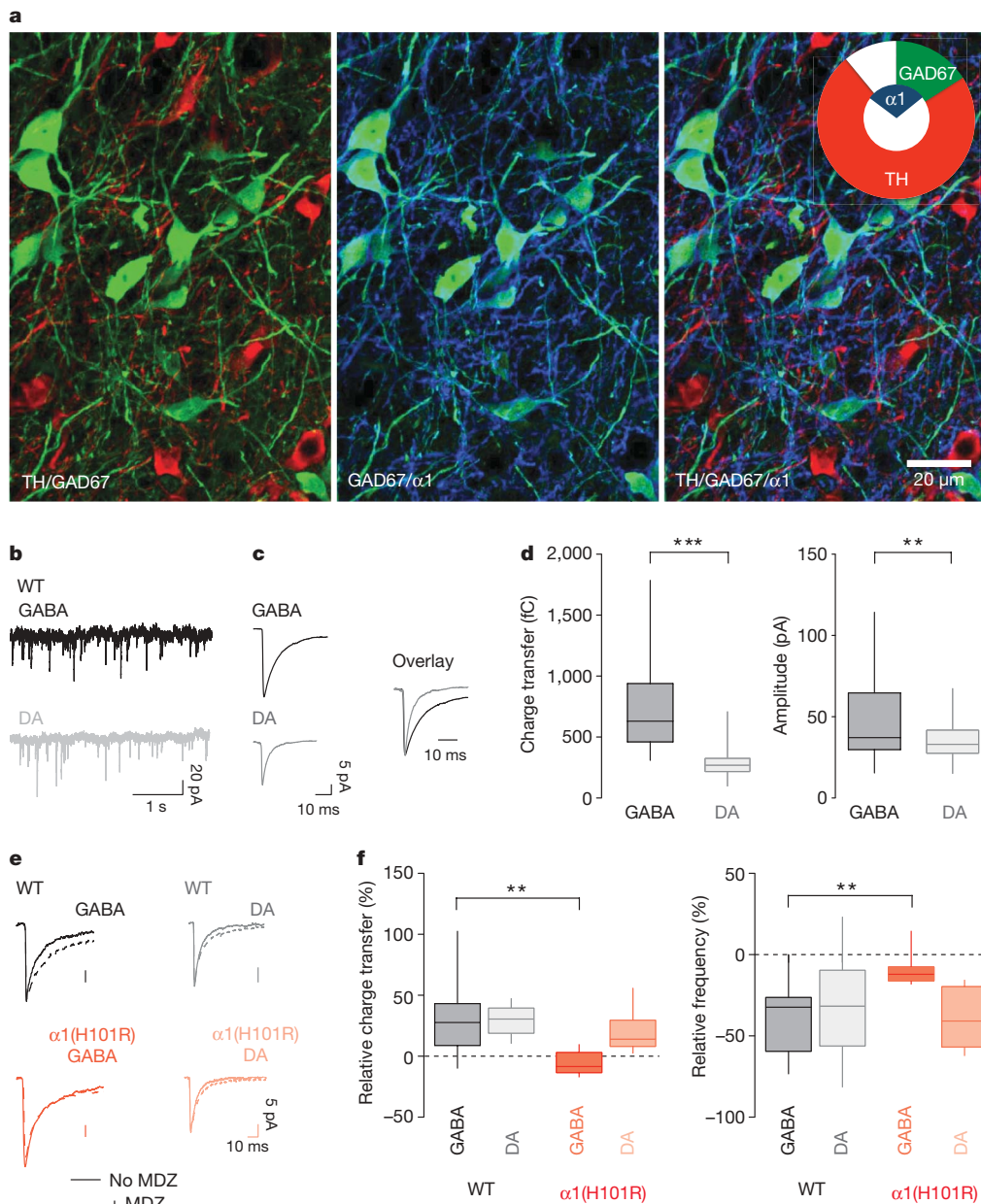


Figure 3 | $\alpha 1$ is selectively expressed in GABA neurons of the VTA. **a**, Immunohistochemical staining for tyrosine hydroxylase (TH, red) and $\alpha 1$ (blue) in VTA slices of GAD67–GFP (green) knock-in mice. Concentric pie charts represent the fraction of $\alpha 1$ -positive cells (inner segment), and quantification of the two cell types (outer segment, $n = 4$ mice). Overlap between inner and outer segments represents colocalization. **b**, Example trace of mIPSC recordings in GABA and DA neurons obtained in slices from wild-type mice. **c**, Representative averaged mIPSC trace from a GABA and a DA neuron. The overlay shows the difference in kinetics when the two currents are normalized to the average mIPSC peak amplitude. **d**, Box plots represent group data for charge transfer and amplitude of mIPSCs obtained from GABA and DA neurons in slices from wild-type mice. The box represents the median and interquartile range, the top and bottom vertical bars denote the 90th and 10th percentile. $t_{(75)} = 7.55$ and $t_{(75)} = 3.16$, respectively; $n = 25$ –48. **e**, Representative average traces of mIPSCs before (solid line) and after (dotted line) application of MDZ (100 nM) in slices from wild-type and $\alpha 1$ (H101R) mice. **f**, Corresponding box-plots representing group data for relative increase in charge transfer and frequency after MDZ bath-application. $t_{(14)} = 3.06$ and $t_{(14)} = 3.23$; $n = 6$ –10. Data are mean \pm s.e.m.; ** $P < 0.01$, *** $P < 0.001$.

genotypes. In GABA neurons, MDZ increased the charge transfer and decreased mIPSC frequency in slices from wild-type mice, but was without effect on mIPSCs recorded in slices from $\alpha 1$ (H101R) mice (Fig. 3e, f and Supplementary Fig. 5a). As expected, MDZ had no effect on mIPSC amplitude in either cell type or genotype¹⁹ (Supplementary Fig. 5b). The observation that the mIPSC frequency is reduced by BDZs except in GABA neurons of $\alpha 1$ (H101R) mice is surprising at first, but could reflect presynaptic GABA_ARs. In fact, such receptors have been described in the VTA, which after activation reduce the release probability²⁰.

Because DA neurons express a set of many subunit isoforms¹¹, the identification of the molecular composition of the GABA_ARs is difficult. Most DA neurons actually express the $\alpha 3$ subunit isoform (96%, Supplementary Fig. 6). Notably, most GABA neurons do not express the $\alpha 3$ subunit isoform (70%) even though significant heterogeneity was observed. In heterologous expressed systems, currents of $\alpha 1$ -containing receptors are smaller than those of $\alpha 3$ -containing receptors²¹. This, however, does not apply to DA neurons in the VTA, because in $\alpha 3$ knockout mice currents are reduced by only 50%²². Our results establish that in $\alpha 1$ (H101R) mice, endogenous GABA_A-mediated synaptic transmission is normal, whereas the

positive modulation of MDZ is abolished in GABA neurons, because the $\alpha 1$ subunit isoform is selectively expressed in these cells.

Cellular determinants of disinhibition

In wild-type mice, mIPSCs in both GABA and DA neurons were enhanced by BDZs. However, when BDZs are administered while transmission is intact, the extent of current amplification in DA neurons depends on the frequency of synaptic events, which originate in the interneurons upstream. We therefore monitored the effect of MDZ on spike-driven, spontaneous IPSCs (sIPSCs) in DA neurons (Fig. 4). Although, the charge transfer of sIPSCs on average increased after MDZ (in line with the mIPSC data), there was a strong reduction of the frequency of spike-driven events in DA neurons (Supplementary Fig. 7). As a result, when we integrated the charge transfer of sIPSCs over time before and after the application of MDZ (relative total current), we found a significant decrease (Fig. 4b). Because interneurons are efficiently inhibited by MDZ, fewer spikes are generated, strongly decreasing the number of sIPSCs, an effect that predominates over the MDZ amplification of the individual event. In $\alpha 1$ (H101R) mice, in contrast, we observed an increased total current in DA neurons because the GABA neurons were insensitive to MDZ. In summary, in wild-type

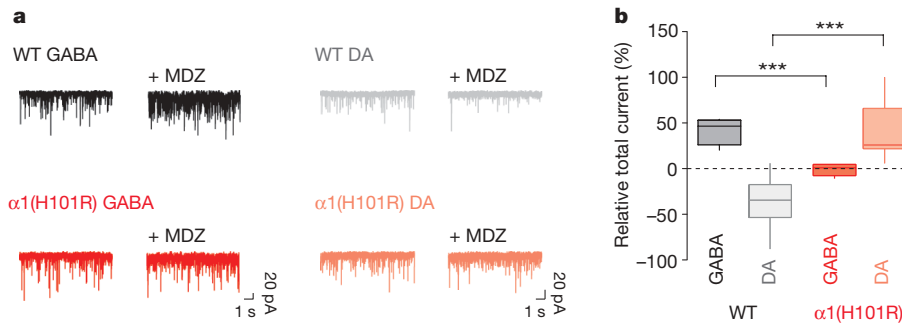


Figure 4 | The total current generated by sIPSCs in DA neurons is decreased by MDZ. **a**, Example trace of sIPSC recordings in GABA and DA neurons obtained before and after application of MDZ in slices from wild-type and $\alpha 1$ (H101R) mice. sIPSCs were abolished with picrotoxin (100 μ M, not shown). **b**, Group data for the relative increase in the overall charge

mice, MDZ led to a net decrease of the total inhibitory current in DA neurons, which could be sufficient to cause their disinhibition (see Supplementary Fig. 1 for schematics).

We therefore tested the effect of MDZ on the firing rate of DA neurons in the VTA by performing extracellular single-unit recordings *in vivo*. When the drug was injected into the tail vein of wild-type mice, we recorded a significant increase in the firing rate that was reversed by flumazenil (Fig. 5a, e, g). In stark contrast, no such disinhibition could be observed in $\alpha 1$ (H101R) mice (Fig. 5b, e, g). In line with a disinhibition model, the data in the DA neurons were mirrored by the observations in GABA neurons. MDZ caused an inhibition of the spontaneous firing rates, at times leading to complete spike suppression (Fig. 5c, f, g). In $\alpha 1$ (H101R) mice, MDZ did not significantly affect firing in GABA neurons (Fig. 5d, f, g). The specificity of these findings are further demonstrated by the observation that in mice in which a different α subunit isoform had been mutated ($\alpha 3$ (H126R) mice)²³, MDZ caused an increase in the firing rate of DA neurons comparable to wild-type mice (Supplementary Fig. 8). The magnitude of this increase was inversely related to the basal firing rate, which further indicates a disinhibition model (Fig. 5e). Moreover, in $\alpha 1$ (H101R) mice, disinhibition of DA neurons was observed with morphine, an effect that was also inversely correlated to the basal firing rate (Fig. 5h). Although anaesthesia may modify the overall distribution of firing rates and therefore the magnitude of the disinhibition, the mean basal firing rates observed here were comparable to values recorded in freely moving animals^{24,25}.

Self-administration of midazolam

The results demonstrate that $\alpha 1$ -containing GABA_ARs mediate the increase of mesolimbic DA in response to BDZs. Furthermore, DA antagonists can reduce self-administration of and preference to these drugs^{26,27}. We therefore tested the effect of the $\alpha 1$ subunit isoform on oral self-administration of MDZ, by offering the mice a free choice of two drinking solutions (Fig. 6a). During the first 3 days the two bottles contained water. Sucrose was then added to both bottles to mask any bitter tastes. This led to an increase in the overall consumption, but no particular preference. Finally, MDZ was added to one of the two bottles. During the test period with MDZ, the total consumption did not change in either genotype (Fig. 6b). A preference for the MDZ solution developed rapidly in wild-type mice, but not in $\alpha 1$ (H101R) mice (Fig. 6c, d). Wild-type mice drank between 0.8 and 1.1 mg kg⁻¹ per 24 h of MDZ, which corresponds to a pharmacological dose. Two control experiments were carried out using a similar protocol. First, we offered $\alpha 1$ (H101R) mice a choice between water and sucrose solution. Both wild-type and mutant mice developed a strong preference for sucrose, indicating that $\alpha 1$ (H101R) mice are not generally deficient in reward reinforcement (Supplementary Fig. 9). We also tested whether $\alpha 3$ (H126R) mice, in which MDZ caused a normal disinhibition of DA neurons (Supplementary Fig. 8), would

transfer (1 min) after MDZ bath-application. Note that in wild-type mice the total current in DA neurons decreases with MDZ application, whereas in $\alpha 1$ (H101R) mice there is an increase. GABA/WT versus GABA/ $\alpha 1$ (H101R) $t_{(9)} = 6.39$, DA/WT versus DA/ $\alpha 1$ (H101R) $t_{(15)} = 5.50$; $n = 6-7$. Box plot designations are as in Fig. 3d; *** $P < 0.001$.

develop a preference for MDZ, which was indeed the case (Supplementary Fig. 10). Although BDZs, particularly MDZ, may enhance taste perception²⁸, this is unlikely to influence the interpretation of these data, as several studies have shown that BDZ-mediated taste enhancement is independent of $\alpha 1$ -containing GABA_ARs^{29,30}.

Discussion

On the basis of our data, we propose that BDZs increase DA levels through disinhibition, similar to opioids, cannabinoids and γ -hydroxybutyrate. This disinhibition is dependent on the BDZ-binding site on $\alpha 1$ -containing GABA_ARs in the VTA. The net effect of BDZs on the VTA circuit is dominated by the role of $\alpha 1$ -containing GABA_ARs, which is supported by the following three observations. First, GABA_AR-mediated quantal transmission is stronger in GABA neurons than in DA neurons, as evidenced by the larger charge transfer of mIPSCs (Fig. 3d). Second, GABA neurons have a higher input resistance than DA neurons¹⁷, allowing the same charge transfer to more effectively change the membrane potential of GABA neurons than DA neurons. Third, the BDZ-dependent enhancement of each IPSC on DA neurons causes little inhibition of DA neuron activity because GABA neurons fall silent and no longer generate those IPSCs. Our model could also apply to earlier work probing the effect of the GABA_AR-agonist muscimol³¹. When administered directly into the VTA, muscimol causes an increase of DA levels in the nucleus accumbens³². This effect only occurs at low doses, which led to the conclusion that the effect is mediated indirectly on non-DA neurons^{33,34}. This inverse dose-dependence may be due to the fact that muscimol, unlike BDZs, is not a positive modulator but an agonist. In line with this interpretation, muscimol at high concentrations in fact inhibits DA neurons³⁵.

The implication of $\alpha 1$ in the addictive effect of BDZs is surprising because the clinically available compound ZOL is selective for this subunit and has been claimed to carry a low risk for addiction³⁶. However, this optimistic view contrasts with the observation that ZOL is readily self-administered³⁷ and the clinical reality. Our data with the subunit isoform-selective compounds also show that ZOL triggers drug-evoked plasticity, and indicate that $\alpha 1$ -sparing compounds may be promising candidates in the search for BDZs devoid of addiction liability. Because $\alpha 1$ -containing GABA_ARs outside the VTA mediate other effects such as seizure control, sedation and anterograde amnesia³⁸, $\alpha 1$ -sparing compounds will certainly not be suitable for all indications. The dissociation between anxiolysis, mainly $\alpha 2$ -mediated²³, and addiction, however, seems possible in principle. This is particularly appealing as high anxiety levels suggest increased vulnerability for addiction³⁹.

Our work unravels the molecular basis of the defining pharmacological features that BDZs share with addictive drugs, which we believe will be key for designing new BDZs with lower addiction liability. However, we note that increased levels of mesolimbic dopamine are necessary for addiction, but not sufficient on their

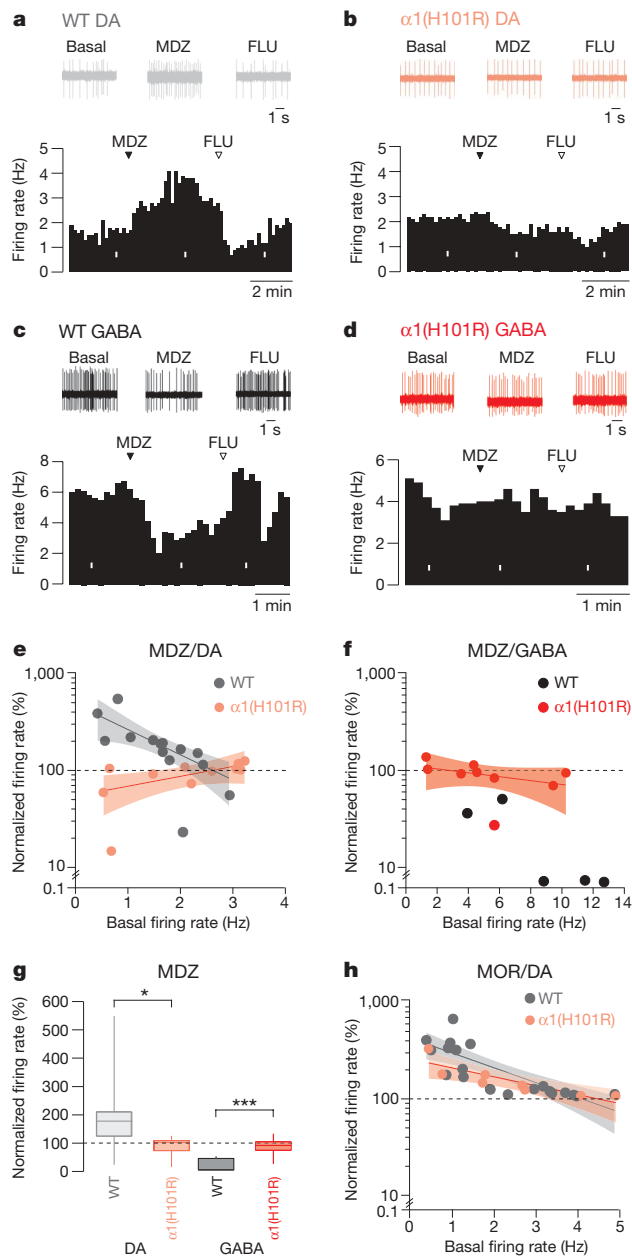


Figure 5 | Opposing effects of MDZ on *in vivo* firing rates of DA and GABA neurons. **a**, Representative extracellular single-unit recording of a DA neuron during the intravenous (i.v.) injection of MDZ (0.5 mg kg⁻¹) in wild-type mice. Corresponding firing frequency plot (bottom panel; flumazenil 1 mg kg⁻¹). **b**, Same experiment in $\alpha 1$ (H101R) mice. **c**, Same experiment as in **a** while monitoring a GABA neuron. **d**, Response of a GABA neuron to MDZ in an $\alpha 1$ (H101R) mouse. White bars indicate time windows of traces shown above. **e**, Normalized firing rate of DA neurons in response to MDZ as a function of the basal activity in wild-type and $\alpha 1$ (H101R) mice. Wild-type/ $\alpha 1$ (H101R) $F_{(2,23)} = 10.63$. **f**, Corresponding plot with the results obtained in GABA neurons. Note that three out of five neurons were completely silenced, which precluded fitting. **g**, Box plots representing group data for relative change in firing rate. Wild-type DA/ $\alpha 1$ (H101R) DA $t_{(23)} = 2.70$, wild-type GABA/ $\alpha 1$ (H101R) GABA $t_{(12)} = 4.60$. Box plot designations are as in Fig. 3d; * $P < 0.05$, *** $P < 0.001$. **h**, Normalized firing rate in response to i.v. injection of morphine (5 mg kg⁻¹) as a function of the basal activity in wild-type and $\alpha 1$ (H101R) mice. Solid lines: regression curves; shaded area: 95% confidence intervals; $n = 5-15$.

own. Recent studies suggest that early drug-evoked plasticity in the VTA may facilitate addiction by gating more enduring forms of adaptations in target regions of the mesolimbic system, which would represent the eventual locus underlying long-term addictive behaviours^{40,41}. Coinciding factors of vulnerability, either in the initial

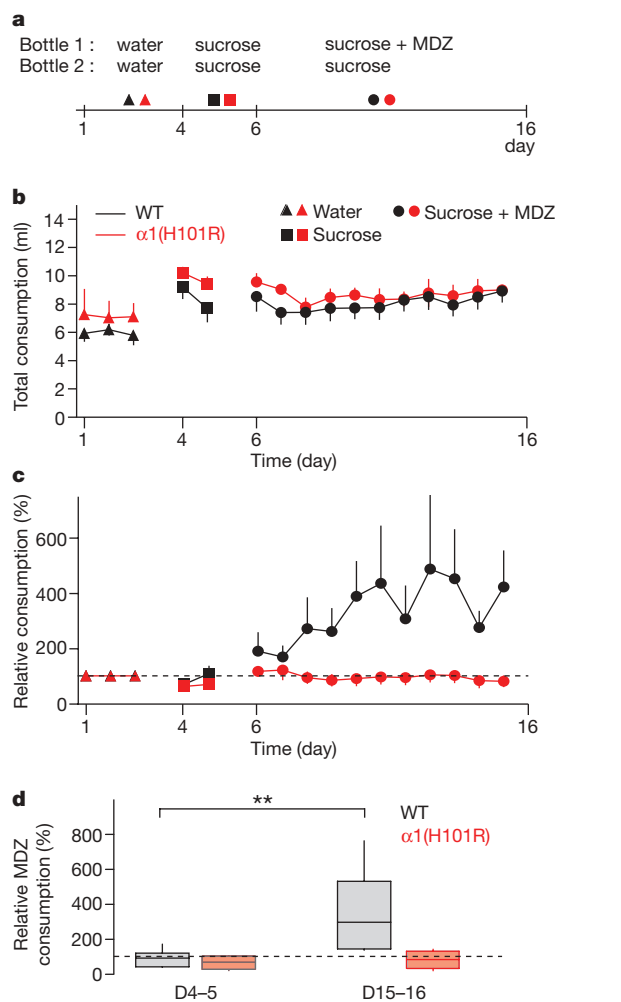


Figure 6 | Oral self-administration of MDZ. **a**, Protocol for behavioural experiment. **b**, Total consumption successively with water, sucrose and MDZ (0.005 mg ml⁻¹) plus sucrose (4%) in wild-type mice (black) and $\alpha 1$ (H101R) (red) mice. Note that wild-type and $\alpha 1$ (H101R) mice drink similar amounts of liquids. **c**, Relative MDZ consumption in wild-type and $\alpha 1$ (H101R) mice. **d**, Corresponding box plots for relative average consumption of MDZ at days (D) indicated. $n = 12-18$ mice in 4-6 cages; $F_{(3,16)} = 5.39$. Box plot designations are as in Fig. 3d; ** $P < 0.01$.

events in the VTA or in subsequent events in mesolimbic targets, may ultimately explain individual variations in susceptibility to addiction, both for BDZs and for other drugs⁴².

METHODS SUMMARY

Horizontal slices of the midbrain (250 μ m) were prepared as previously described⁴³ from C57BL/6 mice, Pitx3-GFP knock-in mice⁴⁴, GAD67-GFP Δ neo mice⁴⁵ and $\alpha 1$ (H101R) knock-in mice¹³, 24 h after i.p. or intra-VTA (mediolateral (ML): ± 0.8 , anteroposterior (AP): -2.4, dorsoventral (DV): -4.4 mm from bregma) injections of different BDZs. AMPAR-mediated EPSCs were recorded in the presence of D(-)-2-amino-5-phosphonovaleric acid (AP5) and picrotoxin. mIPSCs were recorded in the presence of kynurenic acid (2 mM) and tetrodotoxin (500 nM). *In vivo* extracellular single-unit recordings of DA neurons in the VTA (ML: -1.2, AP: -3.2, DV: -4 to 4.5 mm from the bregma) were carried out in wild-type, $\alpha 1$ (H101R) and $\alpha 3$ (H126R)²³ knock-in mice. Drugs were delivered through the tail vein. Immunofluorescence with a guinea-pig antibody against the $\alpha 1$ or $\alpha 3$ subunit, a mouse antibody against tyrosine hydroxylase, and a rabbit antibody against enhanced GFP (eGFP) was performed as previously described¹⁰ in GAD67-GFP Δ neo mice. For the oral self-administration of MDZ, mice were housed with free access to two bottles containing either MDZ in sucrose or sucrose alone. Grouped data are expressed as means \pm s.e.m. For statistical comparisons the one-way analysis of variance (ANOVA), Bonferroni matched, or the paired Student's *t*-tests were used. The levels of significance are indicated as follows: * $P < 0.05$, ** $P < 0.01$ and *** $P < 0.001$.

Full Methods and any associated references are available in the online version of the paper at www.nature.com/nature.

Received 9 July; accepted 2 December 2009.

- Lüscher, C. & Ungless, M. A. The mechanistic classification of addictive drugs. *PLoS Med.* **3**, e437 (2006).
- O'Brien, C. P. Benzodiazepine use, abuse, and dependence. *J. Clin. Psychiatry* **66** (Suppl. 2), 28–33 (2005).
- Saal, D., Dong, Y., Bonci, A. & Malenka, R. C. Drugs of abuse and stress trigger a common synaptic adaptation in dopamine neurons. *Neuron* **37**, 577–582 (2003).
- Bellone, C. & Lüscher, C. Cocaine triggered AMPA receptor redistribution is reversed *in vivo* by mGluR-dependent long-term depression. *Nature Neurosci.* **9**, 636–641 (2006).
- Argilli, E., Sibley, D. R., Malenka, R. C., England, P. M. & Bonci, A. Mechanism and time course of cocaine-induced long-term potentiation in the ventral tegmental area. *J. Neurosci.* **28**, 9092–9100 (2008).
- Mameli, M., Bolland, B., Lujan, R. & Luscher, C. Rapid synthesis and synaptic insertion of GluR2 for mGluR-LTD in the ventral tegmental area. *Science* **317**, 530–533 (2007).
- Heikkinen, A. E., Moykkynen, T. P. & Korpi, E. R. Long-lasting modulation of glutamatergic transmission in VTA dopamine neurons after a single dose of benzodiazepine agonists. *Neuropsychopharmacol.* **34**, 290–298 (2009).
- Johnson, S. W. & North, R. A. Two types of neurons in the rat ventral tegmental area and their synaptic inputs. *J. Physiol. (Lond.)* **450**, 455–468 (1992).
- Sigel, E., Schaerer, M. T., Buhr, A. & Baur, R. The benzodiazepine binding pocket of recombinant $\alpha 1\beta 2\gamma 2$ γ -aminobutyric acid_A receptors: relative orientation of ligands and amino acid side chains. *Mol. Pharmacol.* **54**, 1097–1105 (1998).
- Fritschy, J. M. & Mohler, H. GABAA-receptor heterogeneity in the adult rat brain: differential regional and cellular distribution of seven major subunits. *J. Comp. Neurol.* **359**, 154–194 (1995).
- Okada, H., Matsushita, N., Kobayashi, K. & Kobayashi, K. Identification of GABAA receptor subunit variants in midbrain dopaminergic neurons. *J. Neurochem.* **89**, 7–14 (2004).
- Arendt, R. M., Greenblatt, D. J., Liebisch, D. C., Luu, M. D. & Paul, S. M. Determinants of benzodiazepine brain uptake: lipophilicity versus binding affinity. *Psychopharmacology (Berl.)* **93**, 72–76 (1987).
- Rudolph, U. *et al.* Benzodiazepine actions mediated by specific γ -aminobutyric acid_A receptor subtypes. *Nature* **401**, 796–800 (1999).
- Möhler, H., Benke, D., Mertens, S. & Fritschy, J. M. GABAA-receptor subtypes differing in α -subunit composition display unique pharmacological properties. *Adv. Biochem. Psychopharmacol.* **47**, 41–53 (1992).
- McKernan, R. M. *et al.* Sedative but not anxiolytic properties of benzodiazepines are mediated by the GABA_A receptor $\alpha 1$ subtype. *Nature Neurosci.* **3**, 587–592 (2000).
- Cameron, D. L., Wessendorf, M. W. & Williams, J. T. A subset of ventral tegmental area neurons is inhibited by dopamine, 5-hydroxytryptamine and opioids. *Neuroscience* **77**, 155–166 (1997).
- Margolis, E. B., Lock, H., Hjelmstad, G. O. & Fields, H. L. The ventral tegmental area revisited: is there an electrophysiological marker for dopaminergic neurons? *J. Physiol. (Lond.)* **577**, 907–924 (2006).
- Hsia, A. Y., Malenka, R. C. & Nicoll, R. A. Development of excitatory circuitry in the hippocampus. *J. Neurophysiol.* **79**, 2013–2024 (1998).
- Poncer, J. C., Durr, R., Gähwiler, B. H. & Thompson, S. M. Modulation of synaptic GABA_A receptor function by benzodiazepines in area CA3 of rat hippocampal slice cultures. *Neuropharmacology* **35**, 1169–1179 (1996).
- Long, P. *et al.* Nerve terminal GABAA receptors activate Ca²⁺/calmodulin-dependent signaling to inhibit voltage-gated Ca²⁺ influx and glutamate release. *J. Biol. Chem.* **284**, 8726–8737 (2009).
- Barberis, A., Mozrzymas, J. W., Ortinski, P. I. & Vicini, S. Desensitization and binding properties determine distinct $\alpha 1\beta 2\gamma 2$ and $\alpha 3\beta 2\gamma 2$ GABA_A receptor-channel kinetic behavior. *Eur. J. Neurosci.* **25**, 2726–2740 (2007).
- Yee, B. K. *et al.* A schizophrenia-related sensorimotor deficit links alpha 3-containing GABA_A receptors to a dopamine hyperfunction. *Proc. Natl Acad. Sci. USA* **102**, 17154–17159 (2005).
- Löw, K. *et al.* Molecular and neuronal substrate for the selective attenuation of anxiety. *Science* **290**, 131–134 (2000).
- Robinson, S., Smith, D. M., Mizumori, S. J. & Palmiter, R. D. Firing properties of dopamine neurons in freely moving dopamine-deficient mice: effects of dopamine receptor activation and anesthesia. *Proc. Natl Acad. Sci. USA* **101**, 13329–13334 (2004).
- Hyland, B. I., Reynolds, J. N., Hay, J., Perk, C. G. & Miller, R. Firing modes of midbrain dopamine cells in the freely moving rat. *Neuroscience* **114**, 475–492 (2002).
- Pilotta, R., Singer, G. & Overstreet, D. Self-injection of diazepam in naive rats: effects of dose, schedule and blockade of different receptors. *Psychopharmacology (Berl.)* **84**, 174–177 (1984).
- Fuchs, V., Burbes, E. & Coper, H. The influence of haloperidol and aminoxyacetic acid on etonitazene, alcohol, diazepam and barbital consumption. *Drug Alcohol Depend.* **14**, 179–186 (1984).
- Berridge, K. C. & Pecina, S. Benzodiazepines, appetite, and taste palatability. *Neurosci. Biobehav. Rev.* **19**, 121–131 (1995).
- Yerbury, R. E. & Cooper, S. J. Novel benzodiazepine receptor ligands: palatable food intake following zolpidem, CGS 17867A, or Ro23–0364, in the rat. *Pharmacol. Biochem. Behav.* **33**, 303–307 (1989).
- Morris, H. V., Nilsson, S., Dixon, C. I., Stephens, D. N. & Clifton, P. G. $\alpha 1$ - and $\alpha 2$ -containing GABA_A receptor modulation is not necessary for benzodiazepine-induced hyperphagia. *Appetite* **52**, 675–683 (2009).
- Kalivas, P. W., Duffy, P. & Eberhardt, H. Modulation of A10 dopamine neurons by γ -aminobutyric acid agonists. *J. Pharmacol. Exp. Ther.* **253**, 858–866 (1990).
- Xi, Z. X. & Stein, E. A. Nucleus accumbens dopamine release modulation by mesolimbic GABA_A receptors—an *in vivo* electrochemical study. *Brain Res.* **798**, 156–165 (1998).
- Doherty, M. & Gratton, A. Differential involvement of ventral tegmental GABA_A and GABA_B receptors in the regulation of the nucleus accumbens dopamine response to stress. *Brain Res.* **1150**, 62–68 (2007).
- Grace, A. A. & Bunney, B. S. Paradoxical GABA excitation of nigral dopaminergic cells: indirect mediation through reticulata inhibitory neurons. *Eur. J. Pharmacol.* **59**, 211–218 (1979).
- Klitenick, M. A., DeWitte, P. & Kalivas, P. W. Regulation of somatodendritic dopamine release in the ventral tegmental area by opioids and GABA: an *in vivo* microdialysis study. *J. Neurosci.* **12**, 2623–2632 (1992).
- Soyka, M., Bottlender, R. & Moller, H. J. Epidemiological evidence for a low abuse potential of zolpidem. *Pharmacopsychiatry* **33**, 138–141 (2000).
- Rowlett, J. K., Platt, D. M., Lelas, S., Attack, J. R. & Dawson, G. R. Different GABAA receptor subtypes mediate the anxiolytic, abuse-related, and motor effects of benzodiazepine-like drugs in primates. *Proc. Natl Acad. Sci. USA* **102**, 915–920 (2005).
- Rudolph, U. & Möhler, H. GABA-based therapeutic approaches: GABA_A receptor subtype functions. *Curr. Opin. Pharmacol.* **6**, 18–23 (2005).
- Koob, G. F. Dynamics of neuronal circuits in addiction: reward, anti-reward, and emotional memory. *Pharmacopsychiatry* **42** (suppl. 1), S32–S41 (2009).
- Lüscher, C. & Bellone, C. Cocaine-evoked synaptic plasticity: a key to addiction? *Nature Neurosci.* **11**, 737–738 (2008).
- Mameli, M. *et al.* Cocaine-evoked synaptic plasticity: persistence in the VTA triggers adaptations in the NAc. *Nature Neurosci.* **12**, 1036–1041 (2009).
- Redish, A. D., Jensen, S. & Johnson, A. A unified framework for addiction: vulnerabilities in the decision process. *Behav. Brain Sci.* **31**, 415–437 (2008).
- Labouèbe, G. *et al.* RGS2 modulates coupling between GABA_B receptors and GIRK channels in dopamine neurons of the ventral tegmental area. *Nature Neurosci.* **10**, 1559–1568 (2007).
- Zhao, S. *et al.* Generation of embryonic stem cells and transgenic mice expressing green fluorescence protein in midbrain dopaminergic neurons. *Eur. J. Neurosci.* **19**, 1133–1140 (2004).
- Tamamaki, N. *et al.* Green fluorescent protein expression and colocalization with calretinin, parvalbumin, and somatostatin in the GAD67-GFP knock-in mouse. *J. Comp. Neurol.* **467**, 60–79 (2003).

Supplementary Information is linked to the online version of the paper at www.nature.com/nature.

Acknowledgements We thank members of the Lüscher laboratory as well as M. Frerking, M. Serafin and H. Möhler for critical reading of the manuscript. Y. Yanagawa provided the GAD67-GFP Δ neo mouse line, and we thank K. A. Miczek and H. U. Zeilhofer for help with the GABA_A mutant mouse lines. This work is supported by the National Institute on Drug Abuse (NIDA; DA019022; C.L., P. Slesinger), the Swiss National Science Foundation, the Swiss Initiative in Systems Biology (Neurochoice) and the European Commission Coordination Action ENINET (LSHM-CT-2005-19063). The content is solely the responsibility of the authors and does not necessarily represent the official views of the NIDA or the National Institutes of Health.

Author Contributions K.R.T. carried out all *in vitro* electrophysiology experiments. M.B., G.L. and C.Y. contributed equally to the *in vivo* recordings. K.R.T. and C.C. performed the behavioural experiments. J.-M.F. carried out the immunohistochemistry. U.R. generated the mutant mice. C.L. designed the study and wrote the manuscript with the help of all authors.

Author Information Reprints and permissions information is available at www.nature.com/reprints. The authors declare no competing financial interests. Correspondence and requests for materials should be addressed to C.L. (christian.luscher@unige.ch).

METHODS

Animals. Animals used were 2–3-week-old (*in vitro* electrophysiology) and 20–32-week-old (*in vivo* electrophysiology/behaviour) wild-type C57BL/6 mice, Pitx3–GFP knock-in mice⁴⁴, GAD67–GFP Δ neo mice⁴⁵, α 1(H101R) knock-in mice¹³ and α 3(H126R) knock-in mice²³. All procedures were approved by the local ethics committee as well as the cantonal authorities of Geneva.

***In vitro* electrophysiology.** Horizontal slices (250- μ m thick) of the midbrain were prepared as described previously⁴³. Slices were kept in ACSF containing (in mM) 119 NaCl, 2.5 KCl, 1.3 MgCl₂, 2.5 CaCl₂, 1.0 NaH₂PO₄, 26.2 NaHCO₃ and 11 glucose, and bubbled with 95% O₂ and 5% CO₂. The whole-cell voltage-clamp recording technique was used (31–33 °C, 2 ml min⁻¹, submerged slices) to measure synaptic responses of DA neurons, mIPSCs and holding currents of DA or GABA neurons of the VTA. The holding potential was -60 mV and the access resistance was monitored by a hyperpolarizing step to -90 mV with each sweep every 10 s. Experiments were terminated if the access resistance varied more than 20%. Synaptic currents were evoked by stimuli (0.1 ms) at 0.05 Hz through bipolar stainless steel electrodes positioned rostral to the VTA. When EPSCs were recorded, the internal solution was composed of (in mM) 130 CsCl, 4 NaCl, 2 MgCl₂, 1.1 EGTA, 5 HEPES, 2 Na₂ATP, 5 Na₂-creatine-phosphate, 0.6 Na₃GTP and 0.1 spermine, whereas for mIPSCs the internal solution used contained 30 potassium-gluconate, 100 KCl, 4 MgCl₂, 1.1 EGTA, 5 HEPES, 3.4 Na₂ATP, 10 creatine-phosphate and 0.1 Na₃GTP. Currents were amplified (Multiclamp 700A, Molecular Devices), filtered at 1 kHz and digitized at 5 kHz (National Instruments Board PCI-MIO-16E4, Igor, WaveMetrics). As the liquid junction potential was -3 mV, traces were not corrected. Recordings of EPSCs were carried out in the presence of picrotoxin (100 μ M) and AP5 (50 μ M). The rectification index was calculated by dividing the amplitude of the AMPAR-EPSCs measured at -65 mV by the amplitude at +35 mV. sIPSCs were recorded with continuous bath-application of kynuric acid (2 mM), and tetrodotoxin (500 nM) was added to measure mIPSCs. When sIPSCs were recorded (Fig. 4), the bath-applied ACSF contained a Ca²⁺/Mg²⁺ ratio of 3–6. The goal was to increase the number of interneuronal spikes while interfering with the GABAergic output per spike as little as possible. The multiplicity factor was calculated following the protocol described previously¹⁸. At the end of each experiment, picrotoxin (100 μ M) was bath-applied to verify that the recorded current was mediated by GABA_ARs.

***In vivo* electrophysiology.** Mice were initially anaesthetized with 4% chloral hydrate (480 mg kg⁻¹, i.p.), and supplemented each hour with a lower dose (120 mg kg⁻¹ i.p.) to maintain optimal anaesthesia throughout the experiment. Animals were positioned in a stereotaxic frame (MyNeuroLab) and body temperature was maintained at 36–37 °C using a feedback-controlled heating pad (Harvard Apparatus). An incision was made in the midline to expose the skull. A burr hole was unilaterally drilled above the VTA (AP: -3.0 to 3.4, ML: -1.1 to 1.4, DV: -4 to 4.5 mm from the bregma)⁴⁶, and the dura was carefully retracted. Electrodes were broken back to give a final tip diameter of 1–2 μ m and filled with 2% Chicago Sky Blue dye in 0.5 M sodium-acetate. All electrodes had impedance of 15–25 M Ω . They were angled by 10° from the vertical, slowly lowered through the burr hole with a micro drive (Luigs Neumann) and positioned in the VTA. All electrode descents within a single animal were a minimum of 100 μ m apart. A reference electrode was placed in the subcutaneous tissue. Electrical signals were AC-coupled, amplified (Neurodata), and monitored in real time using an audio-monitor (homemade). Signals were filtered on-line (Humbug, Quest scientific) and digitized at 20 kHz (for waveform analysis) or 5 kHz (Igor, WaveMetrics). The bandpass filter was set between 0.3 and 5 kHz. Extracellular identification of VTA neurons was on the basis of their location as well as on their established electrophysiological properties (DA neurons: biphasic action potential of more than 1.1 ms duration, firing frequency of 0.5–7 Hz and spike height accommodation

during bursts)^{47,48}. In addition, we discriminated between the two populations using an aversive electrical footshock and response to morphine. The drugs were injected through the tail vein using a cannula. After completion of recordings, Chicago Sky Blue dye was deposited by iontophoresis (-15 μ A, 15 min) to mark the position of the final recording site. At the end of the experiment, the brain was kept at -20 °C in a solution of methyl butane. Fifty-micrometre thick coronal sections were cut on a cryostat, stained with luxol fast blue/cresyl violet and the recording site was verified by light microscopy.

Stereotaxic injection. Wild-type and α 1(H101R) mice were anaesthetized with ketamine (100 mg kg⁻¹) and xylazine (10 mg kg⁻¹). The animal was then placed in a stereotaxic frame (MyNeuroLab). The VTA coordinates were ML: \pm 0.8, AP: -2.4, DV: -4.4 mm from bregma, and verified with ink injections. Five microlitres of an 8 mg ml⁻¹ MDZ solution or 5 μ l ACSF were injected bilaterally over 10 min. The animal was sutured and recovered for 24 h until *in vitro* recordings were made.

Immunohistochemistry. GAD67–GFP Δ neo mice were anaesthetized with nembutal (50 mg kg⁻¹) and perfused transcardially with 4% paraformaldehyde in phosphate buffer. The brain was extracted and post-fixed for 3 h, cryoprotected in 30% sucrose in PBS, frozen, and cut at 40 μ m with a sliding microtome. Triple immunofluorescence with guinea-pig antibody against the α 1 or α 3 subunit, a mouse antibody against tyrosine hydroxylase, and a rabbit antibody against eGFP was performed as previously described¹⁰ in perfusion-fixed transverse sections from the brain of GAD67–GFP Δ neo mice. Images were taken with a laser scanning confocal microscope using a \times 20 (numerical aperture (NA) 0.8) or a \times 63 (NA 1.4) objective, using sequential acquisition of separate channels to avoid cross-talk. The fraction of neurons single- and double-labelled for these markers was assessed pair-wise (for example, α 1/TH or α 3/GAD67–GFP) in four equally spaced sections through the VTA per mouse ($n = 4$) and expressed as a percentage of the total number of cells counted.

Oral self-administration. Mice were habituated to handling for 1 week and housed with free access to two 450-ml plastic bottles in their home cage. Two days before the test, 4% sucrose was added to both bottles. During the test mice had access to bottles containing either MDZ (0.005 mg ml⁻¹) in sucrose or sucrose alone. For the sucrose preference experiment in α 1(H101R) mice, sucrose was compared against water. In cases where mice spontaneously preferred one bottle to another during the pretest phase, MDZ was always added to the least-preferred bottle during the test phase. To determine MDZ preference, the relative consumption of MDZ solution to the control solution was calculated.

Drugs. MDZ, diazepam, flunitrazepam, flumazenil, ZOL and L-838 417 were supplied by Tocris, and morphine-HCl by the pharmacy of the University Hospital of Geneva. Drugs were dissolved in saline for i.p. and i.v. injections, in ACSF for intra-VTA injections, and in dimethyl sulphoxide (DMSO) for bath-applications. The final DMSO concentration was 0.1%.

Statistics. Grouped data are expressed as means \pm s.e.m. or box-plots (median, interquartile, and 90th and 10th percentiles). For statistical comparisons the one-way ANOVA, Bonferroni matched, or the paired Student's *t*-tests were used. The levels of significance are: * $P < 0.05$, ** $P < 0.01$ and *** $P < 0.001$. The Kolmogorov–Smirnov test was used to compare cumulative probability plots.

46. Paxinos, G. & Franklin, K. B. J. *The Mouse Brain in Stereotaxic Coordinates* (Elsevier, 2004).

47. Grace, A. A. & Bunney, B. S. Intracellular and extracellular electrophysiology of nigral dopaminergic neurons—1. Identification and characterization. *Neuroscience* 10, 301–315 (1983).

48. Ungless, M. A., Magill, P. J. & Bolam, J. P. Uniform inhibition of dopamine neurons in the ventral tegmental area by aversive stimuli. *Science* 303, 2040–2042 (2004).